# A variational method for water wave radiation and diffraction problems

By J. A. P. ARANHA[1] AND C. P. PESCE[2]

[1]Department of Naval Engineering, USP, CP 61548, São Paulo, Brazil

[2]Division of Naval and Oceânica Engineering, IPT, CP 7141, São Paulo, Brazil

It is shown that the linear and nonlinear exciting force coefficients, the added mass and radiation damping matrices, and the far-field wave amplitude (reflection and transmission coefficients in the two-dimensional case) can all be written as stationary values of well-defined functionals. As a consequence these quantities can be accurately determined with relatively crude approximations for the diffraction and radiation potentials. Numerical experiments confirm this feature: by inverting a $4 \times 4$ real symmetric matrix the results obtained by Vugts (1968), who computed the added mass and radiation damping matrices for several different geometries, were recovered over the whole range of frequencies.

## 1. Introduction

An important problem in ocean engineering is the interaction between a floating structure and sea waves. As is well known, potential theory can be used in this case and the effect of viscous forces, when relevant, can be incorporated by some semi-empirical formulas. In the context of potential theory one is mainly interested in global quantities, such as the exciting force coefficients due to the effect of linear and nonlinear potentials, the added mass and radiation damping matrices, the far-field wave amplitude (reflection and transmission coefficients in the two-dimensional case), and the drift-force coefficients.

These parameters are thought to depend slightly on the detailed features of the flow field, but existing methods to determine them do not take advantage of this. On the contrary, the widespread tendency seems to be to reconstruct the pressure and flow fields and only afterwards, by integration, to determine these quantities. Relevant examples are the Green-function method, where the potential field is computed on the body's surface by solving an integral equation, or the hybrid element method, where it is essentially computed in a finite portion of the fluid domain.

In the present paper the mathematical formalism of the hybrid element method is used to show that all the above-mentioned quantities can be written as stationary values of well-defined functionals. As a consequence, a relatively crude approximation for the potentials (order-$\delta$ error, $\delta \ll 1$) provides a much better approximation for these quantities (order-$\delta^2$ error). Obviously, as in all variational methods, good results depend on judicious choice of the trial function. In the case under analysis this function should represent some gross features of the flow field and it seems convenient to take it as a proper linear combination of elementary singularities (poles, dipoles, vortex lines), placed within the body. As is well known, these singularities can imitate not only the overall behaviour of the fluid flow but also, if

properly placed, some local features such as, for example, the 'rotation' of the fluid around sharp corners.

In this sense the present variational approach leads to a numerical method that is a blend of finite-element and Green-function methods. The mathematical formulation is taken from the former and the representation of the potential as linear combinations of elementary singularities from the latter. It must be stressed, however, that the essential point here is to show that the above-mentioned quantities can be computed by means of a variational method.

In §2 of this paper the general idea of the variational method is demonstrated for a three-dimensional non-homogeneous problem, simulating an arbitrary $N$th-order problem obtained by means of a perturbation technique. To show the power of the method one must compare its performance to some well-known results in the literature. For this reason the remainder of the work is restricted to two-dimensional linear problems. In §3 the variational method is applied to this class of problems, but some modifications in form, not in essence, are introduced. In this way some more subtle theoretical results, with practical implications, can be deduced. Section 4 presents and discusses numerical results.

## 2. The variational method

The nonlinear free-surface potential flow problem can be transformed, by means of a standard perturbation technique, to an infinite sequence of linear non-homogeneous problems. If $\epsilon$ is the small amplitude parameter, the potential $\phi$ can be expressed by an asymptotic series of form $\phi = \sum_{N-1}^{\infty} \epsilon^N \phi_N$, where $\phi_N(x, y, z, t)$ is called the $N$-order potential. For harmonic waves it is the solution of the following set of linear equations:

$$\text{(i)} \quad \nabla^2 \phi_N = 0, \tag{2.1a}$$

$$\text{(ii)} \quad \frac{\partial \phi_N}{\partial z} = \omega^2 \phi_N + f_N \quad \text{at} \quad z = 0, \tag{2.1b}$$

$$\text{(iii)} \quad \nabla \phi_N \cdot \boldsymbol{n}|_{\partial B} = b_N, \tag{2.1c}$$

$$\text{(iv)} \quad \frac{\partial \Phi_N}{\partial z} = 0 \quad \text{at} \quad z = -h, \tag{2.1d}$$

$$\text{(v)} \quad \text{Radiation condition.} \tag{2.1e}$$

In (2.1) $\omega$ is the non-dimensional frequency for this $N$-order problem, $\partial B$ is the body surface, $z = 0$ the undeformed free surface, $z = -h$ the sea bottom, $b_N$ the $N$-order body boundary condition and $f_N(x, y)$ the free-surface exciting term. The appropriate radiation condition will be discussed later but the *linear* radiation condition is given by the well-known expression

$$\left.\begin{aligned}
\phi_N(r, \theta, z) &\sim H_N(\theta) \frac{\mathrm{e}^{\mathrm{i}K_0 r}}{(K_0 r)^{\frac{1}{2}}} \cosh K_0(z+h), \quad r \to \infty, \\
K_0 \tanh K_0 h &= \omega^2.
\end{aligned}\right\} \tag{2.2}$$

Before (2.1) is analysed it is worth introducing some mathematical definitions and results. Problem (2.1) will be addressed in §2.2 and the variational method in §2.3.

## 2.1. *Mathematical background*

Let $S$ be a smooth surface (cylindrical or spherical, for example) dividing the fluid region into two parts: subregion $A$, inside $S$, with finite volume and where the body is placed; subregion $\bar{A}$, outside $S$, with infinite size. In the finite fluid region $A$ one may consider the class of functions with 'finite energy',[†] where the natural norm (energy norm) is given by

$$\|\phi\| = \left[ \iiint_A (|\nabla\phi|^2 + |\phi|^2)\, dA \right]^{\frac{1}{2}}. \tag{2.3}$$

This class of functions is a Hilbert space denoted by $W_2^{(1)}(A)$ in the specialized literature, see Sobolev (1963) and Ladyzhenskaya & Ural'tseva (1968). If $\Psi \in W_2^{(1)}(A)$, let $\bar{\Psi}$ be its extension to the region $\bar{A}$ defined in the following way: $\bar{\Psi} = \Psi$ on $S$ and $\bar{\Psi}$ is the solution of $(2.1\,a, b, d)$ and $(2.2)$, with $f_N = 0$, in $\bar{A}$. The function $\bar{\Psi}$ is uniquely defined in terms of its boundary value $\Psi$ on $S$ and, furthermore, being the solution of a Dirichlet-like problem, it has continuous derivatives of all orders in $\bar{A}$, see Sobolev (1963, p. 93). If $\partial/\partial n$ indicates the derivative in the direction of the normal to $S$, pointing outwards from $A$, then $\partial\bar{\Psi}/\partial n$ should depend linearly on the boundary value of $\Psi$. In this way a linear operator D can be introduced such that

$$\left. \frac{\partial\bar{\Psi}}{\partial n} \right|_S = D(\Psi), \quad \text{all } \Psi \in W_2^{(1)}(A). \tag{2.4a}$$

An explicit expression for $D(.)$ will be presented in §3, although it must be pointed out here that the derivative $\partial\bar{\Psi}/\partial n$ does not exist, in a strict sense, *on the boundary surface* $S$, for an arbitrary $\Psi \in W_2^{(1)}(A)$. It can be defined only in a weak sense, namely by means of a linear functional

$$L(\phi) = \iint D(\Psi)\,\phi\, dS$$

defined in $W_2^{(1)}(A)$. This linear functional is however continuous in $W_2^{(1)}(A)$ and satisfies the following relation:

$$\left| \iint_S D(\Psi)\,\phi\, dS \right| \leqslant C_1 \|\Psi\|\, \|\phi\|. \tag{2.4b}$$

In $(2.4b)$, $C_1$ is a constant independent of $(\phi; \Psi)$ and since this inequality will be used later a sketch of its proof is given here. Consider a region $\bar{A}_1 \subset \bar{A}$ bounded by $S$ and by a smooth surface $S_1$ on the interior of $\bar{A}$. If $\|\,.\,\|_1$ is the energy norm in $\bar{A}_1$ then

$$\left| \iint_{S_1} \frac{\partial\bar{\Psi}}{\partial n} \bar{\phi}\, dS_1 \right| \leqslant C_2 \|\bar{\Psi}\|_1\, \|\bar{\phi}\|_1,$$

† It can be shown that (2.3) is equivalent to

$$\|\phi\|_E = \left( \iiint_A |\nabla\phi|^2\, dA + \omega^2 \iint_F |\phi|^2\, dF \right)^{\frac{1}{2}},$$

where $F$ is the free surface of $A$ and $\omega > 0$, see Sobolev (1963). Obviously $\|\phi\|_E^2$ is the sum of kinetic and potential (gravity) energy in $A$. For $\omega = 0$, $\|\phi\|_E$ is a seminorm and this is the reason why (2.3) has been used.

since $(\bar{\phi}; \bar{\Psi})$ have derivatives of all orders in $\bar{A}$.[†] From Green's theorem and (2.6) (see below), it follows then that

$$\left| \iint_S \mathrm{D}(\Psi)\,\phi\,\mathrm{d}S \right| \leqslant C_3 \|\bar{\Psi}\|_1 \|\bar{\phi}\|_1$$

and since solutions of Dirichlet-like problems can be bounded from above by the norm of their boundary values (see, for example, Ladyzhenskaya & Ural'tseva 1968, chapter 3), then one should have

$$\{\|\bar{\phi}\|_1 ; \|\bar{\Psi}\|_1\} \leqslant C_4\{\|\phi\| ; \|\Psi\|\}.$$

From these last two inequalities (2.4$b$) follows at once with $C_1 = C_3 C_4^2$.

A symmetry property of operator D can also be demonstrated. In fact, applying Green's theorem to a pair $\{\bar{\phi}; \bar{\Psi}\}$ already defined and using (2.2) the following identity can be obtained:

$$\iint_S \mathrm{D}(\phi)\,\Psi\,\mathrm{d}S = \iint_S \mathrm{D}(\Psi)\,\phi\,\mathrm{d}S, \tag{2.5}$$

where (2.4$a$) and the equality $\{\bar{\phi}; \bar{\Psi}\} = \{\phi; \Psi\}$ on $S$ have been used. In this way a particular extension of elements of $W_2^{(1)}(A)$ to the whole fluid region has been introduced and to complete the mathematical background some other results will be needed. The first result is one of the so-called Sobolev's imbedding theorems (see Sobolev 1963) that, in the present context, can be stated as: if $(\phi; \Psi) \in W_2(A)$ and $\partial A$ is the boundary surface of $A$ (or part of it) then,

$$\left| \iint_{\partial A} \phi\Psi\,\mathrm{d}\,\partial A \right| \leqslant C_5 \|\Psi\| \|\phi\|. \tag{2.6}$$

The above relations are necessary to derive some properties of the bilinear form,

$$G(\phi; \Psi) = \iiint_A \nabla\phi \cdot \nabla\Psi\,\mathrm{d}A - \omega^2 \iint_F \phi\Psi\,\mathrm{d}F - \iint_S \mathrm{D}(\phi)\,\Psi\,\mathrm{d}S, \tag{2.7}$$

that appears naturally in the analysis of (2.1), see §2.2. In (2.7), $F$ is the free surface of $A$ and from this expression and (2.5) it follows at once that $G(.;.)$ is *symmetric*, that is $G(\phi; \Psi) = G(\Psi; \phi)$. Furthermore this bilinear form is well defined in $W_2^{(1)}(A)$ and from (2.3), (2.4$b$) and (2.6) the following inequality is obtained:

$$|G(\phi; \Psi)| \leqslant c\|\phi\| \|\Psi\|, \tag{2.8}$$

where, again, the constant $c$ is independent of $(\phi; \Psi)$.

## 2.2. The weak equation

Since $\bar{A}$ has a regular geometry (it is bounded by the horizontal free and bottom surfaces and by a cylindrical or spherical surface $S$) the solution of (2.1) in $A$ can be determined by analytical means (series expansion, for example). For this reason the formal solution of (2.1) in this region will be considered first.

Let, then, $\phi_N^{(\mathrm{P})}$ be a particular solution of (2.1) in the region $\bar{A}$ satisfying two restrictions: first, $\phi_N^{(\mathrm{P})} = 0$ on $S$; second, it has a proper expression at infinity. Besides an eventual outgoing-wave-like behaviour at infinity[‡] this latter condition may

---

[†] This result can be verified directly from the series expansion for $(\bar{\phi}; \bar{\Psi})$ used in §3.

[‡] A particular solution with a proper behaviour at infinity (bounded, etc.) can be determined by integration. An homogeneous solution, which satisfies (2.2), may then be added to ensure that $\phi_N^{(\mathrm{P})} = 0$ on $S$.

imply a wavenumber correction, proportional to wave amplitude squared, for $N \geqslant$ 3. Notice that here the frequency is assumed given and so Stokes' correction should be used for wavenumbers. With these two restrictions the function $\phi_N^{(P)}$ can be uniquely defined and, since it can be obtained by analytical means, it will be supposed known from here on. Since $\phi_N^{(P)} = 0$ on $S$ then, by construction, $\phi_N = \bar{\phi}_N + \phi_N^{(P)}$ on $\bar{A}$, where $\bar{\phi}_N$ is the extension of $\phi_N$, defined in $A$, to the region $\bar{A}$. But $\partial \phi_N / \partial n$ must be continuous on $S$ (being the solution of Laplace's equation) and from the above expression and (2.4a) it follows that

$$\frac{\partial \phi_N}{\partial n}\bigg|_S = D(\phi_N) + \frac{\partial \phi_N^{(P)}}{\partial n}\bigg|_S. \tag{2.9}$$

Notice that $\phi_N$ is not an arbitrary element of $W_2^{(1)}(A)$ since, being the solution of (2.1), it has derivatives of all orders in $S$. Thus $\partial \bar{\phi}_N / \partial n$ exists, in a strict sense, and expression (2.9) is meaningful for the solution $\phi_N$.

Consider now the solution $\phi_N$ of (2.1) in the finite fluid region $A$. It must satisfy the field equation (2.1a) in $A$, the boundary conditions (2.1b) on the free surface $F$ of $A$, (2.1c) on the body surface and (2.9) on $S$. Multiplying the field equation by an 'arbitrary' function $\Psi$, defined in $A$, and integrating by parts one obtains, with the help of the boundary conditions, the identity $G(\phi_N; \Psi) = V_N(\Psi)$, where $G(.;.)$ is given by (2.7) and

$$V_N(\Psi) = \iint_{\partial B} b_N \Psi \, d\partial B + \iint_F f_N \Psi \, dF + \iint_S \frac{\partial \phi_N^{(P)}}{\partial n} \Psi \, dS. \tag{2.10}$$

Notice that $V_N(.)$ is a continuous† linear functional on $W_2^{(1)}(A)$ ($|V_N(\Psi)| \leqslant V_N \| \Psi \|$) and at this point the diffraction problem (2.1) can be formulated in a *weak form*, namely to determine a $\phi_N \in W_2^{(1)}(A)$ such that

$$G(\phi_N; \Psi) = V_N(\Psi), \quad \text{all } \Psi \in W_2^{(1)}(A). \tag{2.11}$$

In the next section it will be shown that a variant of (2.11) can be associated with the stationarity condition of the related Lagrangian. This gives a clear physical meaning for weak equations of form (2.11).

If $\{v_j; j = 1, \ldots, 6\}$ are the rigid-body modes, denoted by surge, sway, heave, roll, pitch and yaw in the specialized literature, let $\{\phi_j; j = 1, \ldots, 6\}$ be the related radiation potentials. They are solutions of (2.1) with $\{b_N = v_j; f_N = 0\}$ and so also satisfy a weak equation of the form

$$G(\phi_j; \Psi) = V_j(\Psi), \quad \text{all } \Psi \in W_2^{(1)}(A), \tag{2.12}$$

with $V_j(.)$ given by

$$V_j(\Psi) = \iint_{\partial B} v_j \Psi \, d\partial B. \tag{2.13}$$

Let $Q_{j,N}$ be defined by the expression

$$Q_{j,N} = V_j(\phi_N). \tag{2.14}$$

From (2.13) one can check that if $\phi_N$ represents the $N$-order diffraction potential, then $Q_{j,N}$ represents the corresponding exciting force coefficient on the $j$-mode. If, on the other hand, $\phi_N = \phi_l$ is a radiation potential, then the real and imaginary parts of $Q_{j,l}$ determine, apart from an eventual factor $\omega$, the coefficients of the added mass

† For this it suffices to assume that $\{b_N; f_N\}$ are square integrable on $\partial B$ and $F$, respectively. The square integrability of $\partial \phi_N^{(P)} / \partial n$ can also be proven from the analytical properties of solutions of Laplace's equation.

and radiation damping matrices. Therefore (2.14) embodies almost all global coefficients needed to analyse the interaction between a floating structure and sea waves. A small modification of the present formulation enables one to express, in a similar way, the far-field wave amplitude (and so the drift force coefficients). This analysis, however, is postponed until the next section.

### 2.3. The variational method

Let $F_{jN}(.;.)$ be a functional defined in the Cartesian product space $W_2^{(1)}(A) \times W_2^{(1)}(A)$ by the expression†

$$F_{jN}(\phi; \Psi) = \frac{V_N(\phi) V_j(\Psi)}{G(\phi; \Psi)}. \qquad (2.15)$$

It is an easy task to check that $Q_{j,N} = F_{jN}(\phi_j; \phi_N)$ and, furthermore, that $F_{jN}(.;.)$ is stationary at $(\phi_j; \phi_N) \in W_2^{(1)}(A) \times W_2^{(1)}(A)$. In fact, from (2.11), (2.12) and (2.14) it follows that $Q_{j,N} = V_j(\phi_N) = G(\phi_j; \phi_N) = V_N(\phi_j)$. Also, the stationary condition for (2.15) implies the weak equations (2.11) and (2.12) and, reciprocally, if the weak equations are satisfied then the variation $\delta F_{jN}(\phi_j; \phi_N)$ is null.

An approximation for $Q_{j,N}$ can be obtained directly from (2.15) by determining the stationary value of $F_{jN}(.;.)$ restricted to a finite-dimensional space $W_a \subset W_2^{(1)}(A)$. This procedure is analogous to using a Rayleigh quotient to determine approximations for the natural frequencies in a vibrating system. It is an easy task to check that $F_{jN}(.;.)$ will be stationary at a $(\phi_{j,a}; \phi_{N,a}) \in W_a \times W_a$ such that

$$\left. \begin{aligned} G(\phi_{N,a}; \Psi_a) = V_N(\Psi_a), \quad \text{all } \Psi_a \in W_a \subset W_2^{(1)}(A), \\ G(\phi_{j,a}; \Psi_a) = V_j(\Psi_a), \quad \text{all } \Psi_a \in W_a \subset W_2^{(1)}(A). \end{aligned} \right\} \qquad (2.16)$$

The corresponding approximation for $Q_{j,N}$ will be denoted by $Q_{j,N}^{(a)}$ and it is then given by the expression

$$Q_{j,N}^{(a)} = F_{jN}(\phi_{j,a}; \phi_{N,a}). \qquad (2.17a)$$

Some alternative formulas for $Q_{j,N}^{(a)}$ are useful. They can be obtained from (2.15) and (2.16) and are written as follows:

$$Q_{j,N}^{(a)} = V_N(\phi_{j,a}) = V_j(\phi_{N,a}) = G(\phi_{N,a}; \phi_{j,a}). \qquad (2.17b)$$

If the exact solutions $(\phi_N; \phi_j)$ are expressed in the form

$$\phi_N = \phi_{N,a} + \delta\phi_N, \qquad \phi_j = \phi_{j,a} + \delta\phi_j, \qquad (2.18)$$

and $\delta$ is defined by

$$\delta = \max\{\|\delta\phi_N\|; \|\delta\phi_j\|\}, \qquad (2.19)$$

then $\delta$ gauges the error of the approximations $(\phi_{N,a}; \phi_{j,a})$ in the energy norm. Some important relations can be obtained from (2.11), (2.12), (2.16) and (2.18). In fact, taking $\Psi = \Psi_a \in W_a$ in these first two expressions and subtracting them from (2.16) one obtains

$$G(\delta\phi_N; \Psi_a) = G(\delta\phi_j; \Psi_a) = 0, \quad \text{all } \Psi_a \in W_a. \qquad (2.20a)$$

Taking also $\Psi = (\delta\phi_j; \delta\phi_N)$ in (2.11), (2.12), the following identity can be derived with the help of (2.20a):

$$G(\delta\phi_j; \delta\phi_N) = V_N(\delta\phi_j) = V_j(\delta\phi_N). \qquad (2.20b)$$

† Strictly speaking $F_{jN}(.;.)$ is defined only for a pair $(\phi; \Psi)$ such that $G(\phi; \Psi) \neq 0$. If, however, $G(\phi_j; \phi_N) = 0$ then $F_{jN}(\phi_j; \phi_N)$ is well defined and zero, see (2.11), (2.12).

The intention now is to compute the error in the approximation $Q_{j,N}^{(a)}$. From the definition of $Q_{j,N}$ and (2.18) one obtains

$$Q_{j,N} = F_{jN}(\phi_j; \phi_N) = \frac{V_N(\phi_{j,a} + \delta\phi_j)\, V_j(\phi_{N,a} + \delta\phi_N)}{G(\phi_{j,a} + \delta\phi_j; \phi_{N,a} + \delta\phi_N)}$$

$$= \frac{V_N(\phi_{j,a})\, V_j(\phi_{N,a}) + V_N(\delta\phi_j)\, V_j(\phi_{N,a}) + V_N(\phi_{j,a})\, V_j(\delta\phi_N) + V_N(\delta\phi_j)\, V_j(\delta\phi_N)}{G(\phi_{j,a}; \phi_{N,a}) + G(\delta\phi_j; \phi_{N,a}) + G(\phi_{j,a}; \delta\phi_N) + G(\delta\phi_j; \delta\phi_N)}.$$

Using (2.17$b$) and (2.20) in this last expression it can be checked that

$$Q_{j,N} = \frac{(Q_{j,N}^{(a)})^2 + 2Q_{j,N}^{(a)}\, G(\delta\phi_j; \delta\phi_N) + (G(\delta\phi_j; \delta\phi_N))^2}{Q_{j,N}^{(a)} + G(\delta\phi_j; \delta\phi_N)}$$

$$= Q_{j,N}^{(a)} + G(\delta\phi_j; \delta\phi_N).$$

With the help of (2.8) and (2.19) the following inequality can then be derived:

$$|Q_{j,N} - Q_{j,N}^{(a)}| = |G(\delta\phi_j; \delta\phi_N)| \leqslant c\|\delta\phi_j\|\,\|\delta\phi_N\| \leqslant c\delta^2. \tag{2.21}$$

This last expression shows explicitly that if the exciting force coefficients are approximated by (2.17) then an error $\delta$ on the potentials implies an error of order $\delta^2$ in the approximation for $Q_{j,N}$. Or, in short, a relatively crude approximation for the potentials can provide a much better approximation for the exciting force coefficients if they are computed by means of (2.17).

Two points should be observed here. The first is that to determine an approximation for the $N$-order exciting force coefficient, the potential $\phi_N$ need not be computed. It suffices to know an approximation $\phi_{j,a}$, for the radiation problem, to obtain $Q_{j,N}^{(a)} = V_N(\phi_{j,a})$. This is a trivial extension of the so-called 'Haskind relations'† and this fact has been observed by several researchers (see, for example, Molin 1979; Lighthill 1979; Aranha & Pesce 1986). In the present formulation, this kind of Haskind relation has an error of order $\delta^2$, where $\delta$ is defined by (2.19). So not only need $\phi_{N,a}$ not be computed but also the error in $Q_{j,N}^{(a)}$ will be much smaller than the one that would be associated with $\phi_{N,a}$.

The second point to be observed is that it has been called to the author's attention that Bessho (1968), in Japan, has derived a similar variational method. There are two basic differences (as well as the formulation) between his method and the present one. First, Bessho's approach is derived for linear (first-order) problems, where $f_N = 0$; second, the trial functions in Bessho's method must satisfy all conditions in (2.1), apart from the boundary condition on the body surface. It turns out, then, that an eventual extension of Bessho's approach, to cover higher-order problems, would need a Green function for the non-homogeneous problem ($f_N \neq 0$). Since $f_N(x,y)$ changes with the wave incidence angle, Bessho's approach may prove impractical to use in higher-order problems. In this context the present method is more general in scope and more flexible in application, since the trial functions can be arbitrary elements of $W_2^{(1)}(A)$. In particular, simple elementary singularities (poles, dipoles and vortex lines) for unbounded fluid can be used in the present formulation, which can make its application easier. However, the numerical experiments that have been analysed here were restricted to linear two-dimensional problems in deep water, since there are abundant results in the literature for this particular case. For this class of

---

† The weak equations (2.11) and (2.12) show quite clearly that Haskind's relations are nothing more than the 'reciprocity relations' in solid mechanics, known for more than a century. Mathematically they are a consequence of the symmetry of $G(.\,;.)$.

problems the analytic expressions for free-surface elementary singularities are relatively simple and have been used in the present work. In this case, the present method, although using a different formulation, leads essentially to the same result that would be obtained using Bessho's approach.

## 3. Linear two-dimensional problem

In this section the variational method will be applied to a cylindrical body, infinitely long in the $x$-direction and symmetric with respect to the plane $y = 0$. If $b$ is the half-beam of the body and $\bar{b} \geqslant b$, let the plane $y = \bar{b}$ be the surface $S$ introduced in §2, see figure 1.

The finite fluid region $A$ is interior to $S(y < \bar{b})$ and the region $\bar{A}$ coincides with the infinite strip $y > \bar{b}$. Since the linear radiation and diffraction problems can be separated with respect to $y$ into even $(+)$ and odd $(-)$ problems, functions defined in $W_2^{(1)}(A)$ are assumed to be extended to region $y < 0$ in an even or odd manner, preserving continuity on $y = 0$.

The function $\bar{\Psi}(y, z)$, the extension of $\Psi \in W_2^{(1)}(A)$ to the region $\bar{A}$, is the solution of the field equation, bottom, free-surface and radiation conditions and satisfies the equality $\bar{\Psi}(\bar{b}, z) = \Psi(\bar{b}, z)$ on $S$. A general solution of this set of equations in the strip $y > \bar{b}$ can be obtained by the method of separation of variables, which leads naturally to the infinite set of functions

$$
\left.\begin{aligned}
f_0(z) = F_0 \cosh K_0(z+h); \quad & \omega^2 = K_0 \tanh K_0 h, \\
f_n(z) = F_n \cos K_n(z+h); \quad -\omega^2 = K_n \tan K_n h; \quad & n = 1, 2, \ldots.
\end{aligned}\right\} \tag{3.1a}
$$

It is not difficult to check that $\{f_n(z); n = 0, 1, \ldots\}$, being the solutions of a Sturm–Liouville problem, is a complete orthogonal set of functions. Furthermore, the normalizing constants $F_n$ can be chosen in such a way that,

$$
\int_{-h}^{0} f_n(z) f_m(z) \, \mathrm{d}z = \delta_{nm}, \tag{3.1b}
$$

where $\delta_{nm}$ is the Kronecker $\delta$-function. Introducing now the linear functionals

$$
L_n(\Psi) = \int_{-h}^{0} \Psi(\bar{b}, z) f_n(z) \, \mathrm{d}z; \quad n = 0, 1, \ldots, \tag{3.2}
$$

the extension $\bar{\Psi}(y, z)$ of $\Psi \in W_2^{(1)}(A)$ can be written in the form

$$
\bar{\Psi}(y, z) = L_0(\Psi) \, \mathrm{e}^{iK_0(|y|-\bar{b})} f_0(z) + \sum_{n=1}^{\infty} L_n(\Psi) \, \mathrm{e}^{-K_n(|y|-\bar{b})} f_n(z). \tag{3.3}
$$

From the definition $(2.4a)$ it follows that

$$
\mathrm{D}(\Psi) = \frac{\partial \bar{\Psi}}{\partial y}\bigg|_{y=\bar{b}} = iK_0 L_0(\Psi) f_0(z) - \sum_{n=1}^{\infty} K_n L_n(\Psi) f_n(z), \tag{3.4}
$$

where (3.4) is an explicit expression for the operator D. Notice that for $|y| > \bar{b}$ the coefficients in the series (3.3) go to zero exponentially when $n \to \infty$ and so $\bar{\Psi}(y, z)$ has derivatives of all orders in the region $|y| > \bar{b}$. Since $K_n/n = O(1)$ when $n \to \infty$, the

FIGURE 1. Geometry for the two-dimensional problem.

series (3.4) is, in general, non-convergent. This exemplifies why $D(\Psi)$ can be defined only in a 'weak sense', see §2.1. Putting (3.4) into (2.7) one obtains†

$$G(\phi;\Psi) = G_1(\phi;\Psi) - iK_0 L_0(\phi) L_0(\Psi);$$
$$G_1(\phi;\Psi) = \iint_A \nabla\phi \cdot \nabla\Psi \, dA - \omega^2 \int_F \phi\Psi \, dF + \sum_{n=1}^{\infty} K_n L_n(\phi) L_n(\Psi). \qquad (3.5)$$

The *real* bilinear form $G_1(.;.)$ will be used later in this section. It is convenient to introduce, for the linear two-dimensional problem, the following notation: $\{\phi_j(y,z);$ $j = 1,\ldots,4\}$ represent the radiation potentials, namely surge‡ $(v_1 = n_x)$, sway $(v_2 = n_y)$, heave $(v_3 = n_z)$ and roll $(v_4 = -zn_y + yn_z)$. Also $\{\phi_j(y,z); j = 5,6\}$ represent the even and odd parts of the diffraction potential $(v_5 = v_6 = 0)$. If $T$ and $R$ are the transmission and reflection coefficients, respectively, then let $\{A_{0,5}; A_{0,6}; \delta_j, j = 1,\ldots,$ $6\}$ be defined by the expressions

$$A_{0,5} = \tfrac{1}{2}(T+R)\,e^{2iK_0\bar{b}}; \quad \delta_5 = +1,$$
$$A_{0,6} = \tfrac{1}{2}(T\text{-}R)\,e^{2iK_0\bar{b}}; \quad \delta_6 = -1, \qquad (3.6)$$
$$\delta_j = 0; \quad j = 1,2,3,4.$$

With (3.6) it is not difficult to check that the far-field behaviour of $\{\phi_j(y,z); j = 1,\ldots,$ $6\}$ is given by

$$\phi_j(y,z) \sim [(A_{0,j} + \tfrac{1}{2}\delta_j)\,e^{iK_0(|y|-\bar{b})} + \tfrac{1}{2}\delta_j\,(e^{-iK_0(|y|-\bar{b})} - e^{iK_0(|y|-\bar{b})})]f_0(z), \qquad (3.7a)$$

with
$$L_0(\phi_j) = A_{0,j} + \tfrac{1}{2}\delta_j. \qquad (3.7b)$$

Owing to the presence of the incident wave, the potentials $\{\phi_j(y,z); j = 5,6\}$ do not have a pure radiating behaviour at infinity. In these cases the parcel

$$\tfrac{1}{2}\delta_j\,(e^{-iK_0(|y|-\bar{b})} - e^{iK_0(|y|-\bar{b})})f_0(z)$$

† If the water depth is infinite, the series summation in (3.3), (3.4) and (3.5) is transformed into integrals in $K = K_n$.

‡ The surge motion, although not strictly two-dimensional, is considered here for completeness. Also, the incident wave has been multiplied by the phase $\exp(iK_0\bar{b})$ to make the notation more succinct, see (3.7a).

plays the same role as $\phi_N^{(P)}$ did in §2 although $f_N = 0$ here. With this observation one can use directly (2.10) and (2.11) to obtain, with the help of (3.5) and (3.7), the following weak equations ($b_N = v_j; f_N = 0$):

$$G_1(\phi_j; \Psi) = iK_0(A_{0,j} - \tfrac{1}{2}\delta_j)L_0(\Psi) + (1 - |\delta_j|)V_j(\Psi), \left.\begin{array}{c} \\ \\ \end{array}\right\}$$

$$V_j(\Psi) = \int_{\partial B} v_j \Psi \, \mathrm{d}\partial B; \quad j = 1, 2, 3, 4. \tag{3.8}$$

So far the general procedure outlined in §2 has been particularized to the linear two-dimensional problem. There is one point, however, that was left aside there and must be worked out here: to show that the far-field wave amplitudes, $A_{0,j}$, can also be determined by a variational method. In order to do so one must separate the ondulatory part of $\overline{\Psi}(y, z)$, proportional to $L_0(\Psi)$ (see (3.3)), from its evanescent one, motivating the introduction of the following linear subspace of $W_2^{(1)}(A)$:

$$W_e(A) = \{\Psi_e \in W_2^{(1)}(A) : L_0(\Psi_e) = 0\}. \tag{3.9}$$

Elements of $W_e(A)$ will be designated by a suffix e, since their extensions to $\bar{A}$ are evanescent. With the help of the auxiliary functions

$$q^\pm(y, z) = \begin{Bmatrix} 1 \\ y/\bar{b} \end{Bmatrix} f_0(z), \tag{3.10}$$

every $\Psi \in W_2^{(1)}(A)$ can be uniquely written in the form

$$\Psi(y, z) = L_0(\Psi)\, q^\pm(y, z) + \Psi_e(y, z); \quad \Psi_e(y, z) \in W_e(A), \tag{3.11}$$

where the + (or −) sign should be used for an even (or odd) function of $y$. For the 'evanescent' function $\Psi_e$ the kinetic and potential (gravity) energies can be defined in the whole fluid domain and, in particular, it can be easily checked that

$$G(\Psi_e; \Psi_e) = G_1(\Psi_e, \Psi_e) = \iint_{A_\infty} (\nabla \Psi_e)^2 \, \mathrm{d}A_\infty - \omega^2 \int_{F_\infty} \Psi_e^2 \, \mathrm{d}F_\infty, \tag{3.12}$$

where $(A_\infty; F_\infty)$ are, respectively, the entire fluid domain and the corresponding free surface. Notice that $G_1(.;.)$ is a *real* bilinear form and for a *real* $\Psi_e$ the quantity $\tfrac{1}{2}G(\Psi_e; \Psi_e)$ is the Lagrangian, if gravity is the only source of potential energy. These are important consequences of the split between the ondulatory and evanescent parts of $\Psi$ and they will be used later in this section.

Using (3.11) in (3.8) and a similar expression for $\phi_j(y, z)$ (see (3.7b)), the final solution can be expressed in terms of intermediate weak solutions defined in $W_e(A)$. In order to present this result in a more compact form, some definitions are needed. Let then

$$\begin{Bmatrix} V_5(\Psi) \\ V_6(\Psi) \end{Bmatrix} = -G_1(q^\pm; \Psi), \tag{3.13}$$

and consider the set of weak equations: to determine $\{\phi_{j,e} \in W_e(A); j = 1, \ldots, 6\}$ such that

$$G_1(\phi_{j,e}; \Psi_e) = V_j(\Psi_e), \quad \text{all } \Psi_e \in W_e(A), \tag{3.14}$$

with $\{V_j(.); j = 1, \ldots, 6\}$ given by (3.8), (3.13). If now

$$p^\pm(y, z) = q^\pm(y, z) + \begin{cases} \phi_{5,e}(y, z), \\ \phi_{6,e}(y, z), \end{cases} \tag{3.15}$$

then it can be checked, after some algebra, that

$$A_{0,j} = -\tfrac{1}{2}\delta_j \frac{G_1(p^\pm ; p^\pm) + iK_0}{G_1(p^\pm ; p^\pm) - iK_0} + (1 - |\delta_j|)\frac{V_j(p^\pm)}{G_1(p^\pm ; p^\pm) - iK_0}, \tag{3.16a}$$

$$\phi_j(y, z) = (A_{0,j} + \tfrac{1}{2}\delta_j)\, p^\pm(y, z) + (1 - |\delta_j|)\, \phi_{j,\,\mathrm{e}}(y, z). \tag{3.16b}$$

The coefficients $\delta_j$ have been defined in (3.6) and it should be observed that the solution of the six original potential problems has been transformed, essentially, into the solution of the six *real* weak equations (3.14). As will be shown next, these equations have a very neat physical meaning.

To make this point clear, an analogy with a linear discrete system, with restoring matrix $K_{ij}$ and generalized coordinates $q_j$, seems worthwhile. If this discrete system is under the action of external conservative forces $P_j$, then the *total* potential energy is given by

$$U(q_i) = \tfrac{1}{2}\sum\sum K_{ij}\, q_i\, q_j - \sum P_j\, q_j,$$

where the first parcel is the *restoring potential energy* and $\sum P_j q_j$ is the *work done by the external forces on the system*. Consider now the general problem related to (3.14). Here the restoring forces, due to gravity, have potential energy

$$U(\phi_{j,\,\mathrm{e}}) = \tfrac{1}{2}\omega^2 \int_{F_\infty} (\phi_{j,\,\mathrm{e}})^2 \,\mathrm{d}F_\infty.$$

In the $j$-radiation problem, the work done by the fluid pressure on the body is given by

$$V_j(\phi_{j,\,\mathrm{e}}) = \int_{\partial B} \phi_{j,\,\mathrm{e}}\, v_j \,\mathrm{d}\,\partial B,$$

and so the work done by the body on the fluid is $-V_j(\phi_{j,\,\mathrm{e}})$. It follows that the *total* potential energy for the $j$-problem is given by the expression

$$U_j(\phi_{j,\,\mathrm{e}}) = \tfrac{1}{2}\omega^2 \int_{F_\infty} (\phi_{j,\,\mathrm{e}})^2 \,\mathrm{d}F_\infty + V_j(\phi_{j,\,\mathrm{e}}). \tag{3.17a}$$

A similar interpretation, although in a less direct way, is also possible for the diffraction problem, $j = 5, 6$. In fact, in this case the exciting terms are the fields $q^\pm(y, z)$ and the work done by them on the fluid is given by

$$\iint \nabla q^\pm \cdot \nabla \phi_{j,\,\mathrm{e}} \,\mathrm{d}A - \omega^2 \int q^\pm \phi_{j,\,\mathrm{e}} \,\mathrm{d}F = G_1(q^\pm ; \phi_{j,\,\mathrm{e}}) = -V_j(\phi_{j,\,\mathrm{e}}), \quad j = 5, 6.$$

The kinetic energy, associated with the (evanescent) $j$-solution, is clearly given by

$$T(\phi_{j,\,\mathrm{e}}) = \frac{1}{2}\iint_{A_\infty} (\nabla \phi_{j,\,\mathrm{e}})^2 \,\mathrm{d}A_\infty, \tag{3.17b}$$

and, with the help of (3.12) and (3.17 $a, b$), the Lagrangian can be written in the form

$$\mathscr{L}_j(\phi_{j,\,\mathrm{e}}) = T(\phi_{j,\,\mathrm{e}}) - U_j(\phi_{j,\,\mathrm{e}}) = \tfrac{1}{2}G_1(\phi_{j,\,\mathrm{e}}; \phi_{j,\,\mathrm{e}}) - V_j(\phi_{j,\,\mathrm{e}}). \tag{3.17c}$$

In a discrete system, oscillating harmonically in time, one has $q_j(t) = q_{j,0}\,\mathrm{e}^{i\omega t}$ and so $\mathscr{L} = \mathscr{L}(q_j ; \dot{q}_j) = \mathscr{L}(q_{j,0})$. In this circumstance Lagrange's equation of motion reduces to $\partial \mathscr{L}/\partial q_{j,0} = 0$, or, in short, to the stationary condition for the Lagrangian. In a *continuum* system the field $\phi_{j,\,\mathrm{e}}(y, z)$ takes the place of the discrete variables $\{q_{j,0}\}$ and Lagrange's equation of motion is reduced to the stationary condition of (3.17 $c$). The

weak equation (3.14) is just this condition and this gives a physical meaning to this equation.

For future reference some results concerning the functions $p^{\pm}(y, z)$ should be derived here. In fact, if the *real* parameters $\varLambda_{jl}$ are defined by the expressions

$$\varLambda_{jl} = G_1(\phi_{j,\,\mathrm{e}}; \phi_{l,\,\mathrm{e}}) = V_j(\phi_{l,\,\mathrm{e}}) = V_l(\phi_{j,\,\mathrm{e}}), \quad j, l = 1, \ldots, 6, \tag{3.18}$$

then the following identities can be derived:

$$V_j(p^{\pm}) = V_j(q^{\pm}) + \begin{cases} \varLambda_{j5}, \\ \varLambda_{j6}, \end{cases} \tag{3.19a}$$

$$G_1(p^{\pm}; p^{\pm}) = G_1(q^{\pm}; q^{\pm}) - \begin{cases} \varLambda_{55}, \\ \varLambda_{66}. \end{cases} \tag{3.19b}$$

The first one follows from (3.15) and (3.18), and to deduce (3.19b) one observes, from (3.13), (3.14) and (3.15) that $G_1(p^{\pm}; \varPsi_{\mathrm{e}}) = 0$, for all $\varPsi_{\mathrm{e}} \in W_{\mathrm{e}}(A)$. From this last equality, and (3.13), (3.15) and (3.18), one obtains (3.19b).

Let now $\{(m_{jl}; d_{jl}), j, l = 1, \ldots, 4\}$ be the elements of the added mass and radiation damping matrices, $\{Q_l; l = 1, \ldots, 4\}$ be the exciting force coefficients, due to the linear diffraction potential, $\{A_{0,j}; j = 1, \ldots, 4\}$ be the radiation far-field wave amplitude and $\{T; R\}$ be the transmission and reflection coefficients. In the interaction between a floating structure and sea waves one is mostly interested in computing the coefficients $\{m_{jl}; d_{jl}; Q_l; A_{0,j}; T; R\}$ since, with them, the oscillatory motion of the structure, its drift in the horizontal plane or even its performance as a breakwater etc., can all be evaluated.

Since $\{m_{jl}; d_{jl}; Q_l\}$ are defined by means of integrals over the body surface and only half of it is considered here, the integrals should be multiplied by $\varDelta_{jl} = 1 + (-1)^{j+l}$, to make the final result correct. From the basic definitions

$$m_{jl}(\omega) = \varDelta_{jl} \int_{\partial B} (\mathrm{Re}\, \phi_j)\, v_l\, \mathrm{d}\partial B; \quad j, l = 1, \ldots, 4,$$

$$d_{jl}(\omega) = \varDelta_{jl}\, \omega \int_{\partial B} (\mathrm{Im}\, \phi_j)\, v_l\, \mathrm{d}\partial B; \quad j, l = 1, \ldots, 4,$$

$$Q_l(\omega) = \varDelta_{jl} \int_{\partial B} \phi_j\, v_l\, \mathrm{d}\partial B; \quad j = 5, 6, l = 1, \ldots, 4,$$

and (3.16), the following relations can be derived:

$$m_{jl}(\omega) = \varDelta_{jl} \left[ \frac{V_j(p^{\pm})\, V_l(p^{\pm})}{K_0^2 + (G_1(p^{\pm}; p^{\pm}))^2} G_1(p^{\pm}; p^{\pm}) + \varLambda_{jl} \right]; j, l = 1, \ldots, 4, \tag{3.20a}$$

$$d_{jl}(\omega) = \varDelta_{jl}\, \omega K_0 \frac{V_j(p^{\pm})\, V_l(p^{\pm})}{K_0^2 + (G_1(p^{\pm}; p^{\pm}))^2}; \quad j, l = 1, \ldots, 4, \tag{3.20b}$$

$$Q_l(\omega) = -\delta_j \varDelta_{jl}\, \mathrm{i}K_0 \frac{V_l(p^{\pm})}{G_1(p^{\pm}; p^{\pm}) - \mathrm{i}K_0}; \quad j = 5, 6, \quad l = 1, \ldots, 4, \tag{3.20c}$$

$$A_{0,j}(\omega) = \frac{V_j(p^{\pm})}{G_1(p^{\pm}; p^{\pm}) - \mathrm{i}K_0}; \quad j = 1, \ldots, 4, \tag{3.20d}$$

$$T(\omega) = \frac{1}{2} \left[ \frac{G_1(p^-; p^-) + \mathrm{i}K_0}{G_1(p^-; p^-) - \mathrm{i}K_0} - \frac{G_1(p^+; p^+) + \mathrm{i}K_0}{G_1(p^+; p^+) - \mathrm{i}K_0} \right] \mathrm{e}^{-2\mathrm{i}K_0 \bar{b}}, \tag{3.20e}$$

$$R(\omega) = -\frac{1}{2} \left[ \frac{G_1(p^-; p^-) + \mathrm{i}K_0}{G_1(p^-; p^-) - \mathrm{i}K_0} + \frac{G_1(p^+; p^+) + \mathrm{i}K_0}{G_1(p^+; p^+) - \mathrm{i}K_0} \right] \mathrm{e}^{-2\mathrm{i}K_0 \bar{b}}. \tag{3.20f}$$

From (3.19) and (3.20) it follows that $\{m_{jl}; d_{jl}; Q_l; A_{0,j}; T; R\}$ can be determined directly once the real coefficients $\{A_{jl}; j, l = 1, \dots, 6\}$ are computed (recall that $q^{\pm}(y, z)$ are known, see (3.10)). As is clear from (3.18), $A_{jl}$ is a stationary value of the functional $F_{jl}(.;.)$, see (2.15), in the Cartesian product space $W_e(A) \times W_e(A)$. All quantities of interest can, then, be computed by a variational method.

Although the motivation for splitting the functions $\Psi \in W_2^{(1)}(A)$ into 'ondulatory' and 'evanescent' parts was to obtain a variational method to compute $\{A_{0,j}; T; R\}$, some by-products of this procedure should be emphasized here. In fact, not only are the weak equations (3.14) real, which makes the numerical solutions more economic, but also these equations can then be interpreted in a very clear physical way. Furthermore, it makes it possible to write $m_{jl}; d_{jl}$, etc. in the form (3.20) and, from the structure of these formulas, some interesting results can be derived.

The first is that there are several identities, known as 'reciprocity relations' and 'energy theorems', associated with both the diffraction and radiation problems. Relevant examples are: energy conservation $|R|^2 + |T|^2 = 1$; Haskind relations between the exciting forces $Q_l(\omega)$ and the coefficients $A_{0,l}(\omega)$; the equality between the phases of the even (or odd) coefficients $A_{0,1}, A_{0,3}$ (or $A_{0,2}, A_{0,4}$), etc. *All* these relations can be obtained directly from (3.20) and, furthermore, they depend only on the structure of these expressions. In particular, if the potentials are approximated by any numerical method then, no matter how bad the approximations are, these identities will be exactly satisfied if (3.20) is employed. Or, in short, the energy theorem, Haskind's relation, etc., cannot be used to assess the discretization error of the approximation, a result already derived by Aranha, Mei & Yue (1979) in a less direct way. This fact is strictly valid only if (3.20) is used but it strongly indicates that the checking of these identities should never be taken seriously as a convergence criterion.

Another interesting conclusion can be derived from (3.20b). This expression shows that not only the radiation damping matrix is positive semidefinite but, in fact, it is *always* singular. A physical explanation of this result is provided by (3.20d): if, for example, $(\xi_2; \xi_4)$ are the non-dimensional sway and roll amplitudes and $\xi_2/\xi_4 = -V_4(p^-)/V_2(p^-)$, then the far-field wave amplitude generated by this coupled motion is zero.

A similar conclusion concerning the sign of the added mass matrix is not possible, in general, but for an important class of geometries an affirmative answer can be obtained. Let a W-body be the class of bodies whose projection on the free-surface coincides with its water line. The one shown in figure 1 is not a W-body but those shown in figure 2 are. For a W-body a finite fluid region $A$ can be defined without a free surface (take $b = \bar{b}$) and, from (3.5), $G_1(\phi; \phi)$ is strictly positive in this case. From (3.19) and (3.20a) it follows then that the added mass matrix is positive definite for a W-body. A physically interesting discussion on negative added mass for a particular non-W-body can be found in Newman, Sortland & Vinje (1984).

## 4. Numerical results

The purpose of this section is to discuss the numerical results obtained from the variational method and compare them with some obtained from more standard numerical procedures. Typical geometries (circular, rectangular and triangular, see figure 2) in deep water will be analysed and the results compared to Vugts (1968). In §4.1 attention is focused on the convergence of the method and, for this, poles are placed within the body in increasing number, imitating the well-known Green-
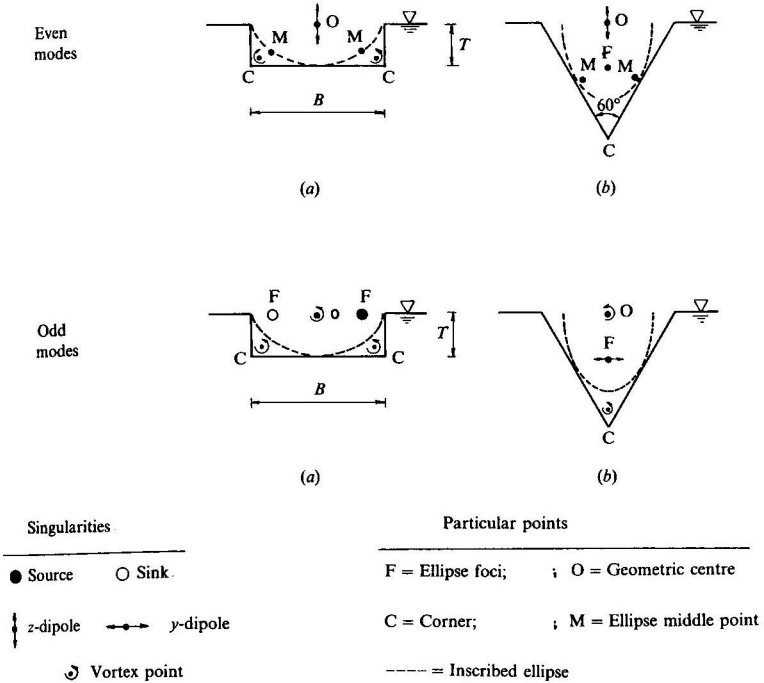
FIGURE 2. Geometries analysed in this section and singularities used in the variational approximation. Vortex point at $O$ simulates roll boundary condition (figure $3b$); vortex point at $C$ simulates corner's effect (figure $3a, c$).

function method. Although convergence is relatively fast this procedure does not exploit the flexibility and intrinsic properties of the variational method. On one hand, this method allows all sorts of singularities – and not only poles – to be used simultaneously; on the other hand, a variational approach works better if the chosen trial functions are able to imitate some gross physical features of the problem under consideration. In §4.2, some well-known features of the fluid flow around a floating body are discussed and some simple trial functions, that simulate such a behaviour, are then introduced. Their performances are analysed in some detail in §4.3, where rectangular cross-sections are studied, and in §4.4 numerical results obtained for a triangular cross-section are presented. Finally, §4.5 gives more results related to transmission, reflection and exciting forces coefficients.

### 4.1. *Convergence of the method*

To verify numerically the convergence of the method a sequence of approximations was constructed. Poles were spread over a line $\partial B^*$ within the body, with length $L_B^*$ and parallel to $\partial B$. The number and position of poles have been defined in the following way: for the first approximation, two poles separated by $L_B^*$; for the second, three poles separated by $L_B^*/2$; for the $n$th, $2^{n-1}+1$ poles separated by $L_B^*/2^{n-1}$; etc. Since a function $T_0^{\pm}(y, z)$, to be defined in the next subsection, was used in all approximations, this construction generates a sequence of finite-dimensional

| $\omega$ | $(3 \times 3)$ | $(4 \times 4)$ | $(6 \times 6)$ | $(10 \times 10)$ |
|------|--------|--------|--------|----------|
| 0.25 | 1.6920 | 1.7360 | 1.7497 | 1.7505 |
| 0.50 | 0.8318 | 0.8641 | 0.8777 | 0.8785 |
| 0.75 | 0.5906 | 0.6080 | 0.6231 | 0.6241 |
| 1.00 | 0.5897 | 0.5896 | 0.6046 | 0.6057 |
| 1.25 | 0.6560 | 0.6548 | 0.6727 | 0.6740 |
| 1.50 | 0.6982 | 0.7098 | 0.7433 | 0.7537 |
| 1.75 | 0.6481 | 0.7625 | 0.8147 | 0.8184 |
| 2.00 | 0.6829 | 0.8131 | 0.8621 | 0.8649 |

TABLE 1. Successive approximations for the heave added mass of a circle. $\omega = \tilde{\omega}(B/2g)^{\frac{1}{2}}$; $B = $ beam

| $\omega$ | $A_{0,5}$ | | | | $A_{0,6}$ | | | |
|------|--------|--------|--------|----------|--------|--------|--------|----------|
| | $(3 \times 3)$ | $(4 \times 4)$ | $(6 \times 6)$ | $(10 \times 10)$ | $(3 \times 3)$ | $(4 \times 4)$ | $(6 \times 6)$ | $(10 \times 10)$ |
| 0.25 | $-5.6$ | $-5.6$ | $-5.5$ | $-5.5$ | 7.4 | 7.4 | 7.4 | 7.4 |
| 0.50 | $-15.2$ | $-15.1$ | $-14.5$ | $-14.4$ | 31.4 | 31.5 | 31.7 | 31.8 |
| 0.75 | $-23.3$ | $-22.6$ | $-20.7$ | $-20.2$ | 68.6 | 69.3 | 70.4 | 71.1 |
| 1.00 | $-28.5$ | $-26.7$ | $-22.7$ | $-21.7$ | 103.0 | 105.0 | 108.0 | 110.0 |
| 1.25 | $-30.8$ | $-27.5$ | $-21.3$ | $-19.6$ | 128.0 | 131.0 | 134.0 | 136.0 |
| 1.50 | $-29.6$ | $-24.9$ | $-17.9$ | $-15.7$ | 144.0 | 148.0 | 151.0 | 153.0 |
| 1.75 | $-27.7$ | $-19.3$ | $-13.8$ | $-11.4$ | 155.0 | 160.0 | 162.0 | 164.0 |
| 2.00 | 81.8 | $-12.8$ | $-9.8$ | $-7.6$ | $-18.1$ | 168.0 | 169.0 | 170.0 |

TABLE 2. Successive approximations for the phase (degrees) of the coefficients $A_{0,5}, A_{0,6}$, for a $B/T = 8.0$ rectangle. $\omega = \tilde{\omega}(B/2g)^{\frac{1}{2}}$, $B = $ beam

spaces $\{W_{e,1} \subset W_{e,2} \subset \ldots \subset W_{e,n} \subset \ldots \subset W_e(A)\}$ with dimensions $\{3 < 4 < \ldots < 2^{n-1} + 2 < \ldots < \infty\}$. Obviously the dimension of $W_{e,n}$ corresponds to the size of the real and symmetric matrix that must be constructed and inverted in the $n$th approximation. In all numerical experiments the non-dimensional distance between $\partial B^*$ and $\partial B$ was 0.125, or 6.25% of the beam.

Table 1 presents the results for the heave added mass of the circle and each approximation is identified by the size of the related matrix. The last column in the table agrees with Vugts (1968), the convergence of successive approximations being quite evident.

For three different geometries (two rectangles and a triangle), similar results as for the hydrodynamic coefficients have been obtained; see Pesce (1988) for details. An example is given in table 2, where the convergence for the phases of the wave amplitude coefficients $(A_{0,5}; A_{0,6})$ is shown, for a rectangle with beam/draught $= 8.0$. These results will be used later.

For this particular sequence of approximations the following general rule can be derived: a $(6 \times 6)$ numerical solution gives a result good enough for practical purposes. This performance should be compared to the usual Green-function method, where a typical $(25 \times 25)$ complex non-symmetric matrix must, in general, be constructed and inverted, see Nestegård & Sclavounous (1984). As already mentioned, the approximations under consideration do not explore the flexibility and intrinsic properties of the variational method. The next subsection discusses this point, introducing more convenient trial functions.

### 4.2. *Choice of convenient trial functions*

The potentials $\{\phi_j(y,z); j = 1, \ldots, 6\}$ can be written in the form (3.16 b) or, in a more explicit way, as

$$\left.\begin{aligned}
\phi_j(y,z) &= A_{0,j}\,p^{\pm}(y,z) + \phi_{j,\mathrm{e}}(y,z); j = 1, \ldots, 4,\\
\phi_j(y,z) &= (A_{0,j} - \tfrac{1}{2}(-1)^j)\,p^{\pm}(y,z); \quad j = 5, 6.
\end{aligned}\right\} \tag{4.1}$$

A glance at (4.1) indicates that the real function $p^{+}(y,z)$ (or $p^{-}(y,z)$) corresponds, apart from a constant factor, to the even (or odd) part of the diffraction potential. In order to make the notation more succinct they will be called 'diffraction potentials'. The interesting aspect of (4.1) is that the radiation potentials have been naturally split into two parts: the first proportional to the 'diffraction potentials' $p^{\pm}(y,z)$, with zero normal derivative on the body surface; the other a *real evanescent* function $\phi_{j,\mathrm{e}}(y,z)$ satisfying the mode boundary condition (surge, sway, heave, roll) on the body surface.† Appropriate trial functions should then simulate the gross behaviour of $\{p^{\pm}(y,z); \phi_{j,\mathrm{e}}(y,z), j = 1, \ldots, 4\}$, whose physical meaning has been just discussed.

Consider first the diffraction potential $p^{\pm}(y,z)$. Part of these functions are given respectively by the even and odd components of the incident wave $\{\cos K_0 y; \sin K_0 y\} f_0(z)$. Furthermore, from the Froude–Krilov approximation,

$$p^{\pm}(y,z) \sim \{\cos K_0 y; \sin K_0 y\} f_0(z)$$

in the limit $\omega \to 0$ and, when $\omega \to \infty$, both $p^{\pm}(y,z)$ and $\{\cos K_0 y; \sin K_0 y\} f_0(z)$ are essentially zero for $z < 0$. It seems desirable, then, to use trial functions that can recover, at least, the pure incident wave behaviour. This can be done if the weak equations (3.14) are solved, for $j = 5, 6$, in the absence of any obstacle. In this case it is an easy task to show that $\{\phi_{j,\mathrm{e}}(y,z); j = 5, 6\}$ are proportional to the functions

$$\left.\begin{aligned}
T_0^{+}(y,z) &= (\cos K_0 y - \cos K_0 b) f_0(z),\\
T_0^{-}(y,z) &= (\sin K_0 y - \frac{y}{b}\sin K_0 b) f_0(z).
\end{aligned}\right\} \tag{4.2}$$

These trial functions simulate the correct behaviour of the evanescent diffraction potentials $\{\phi_{j,\mathrm{e}}(y,z); j = 5, 6\}$ in the limits $\omega \to 0$ or $\omega \to \infty$ and it is not difficult to check, placing (4.2) into (3.20), that they recover the correct asymptotic behaviour of $\{R(\omega); T(\omega)\}$ in these limits. In the intermediate range of frequencies the use of $T_0^{\pm}(y,z)$ is not sufficient to provide a proper result. The performance can, however, be improved if other trial functions, to be derived next, are employed. Obviously the same $T_0^{\pm}(y,z)$ should also be used for radiation problems, since these potentials depend on $p^{\pm}(y,z)$.

To analyse the radiation potentials $\{\phi_{j,\mathrm{e}}(y,z); j = 1, \ldots, 4\}$ it seems natural to consider first a *circular* cross-section. In the limit $\omega \to 0$, surge and heave motions represent a body dilatation and they can be simulated by a pole placed at the circle centre. Incidentally, it is not difficult to show that, for any surface-piercing body, the correct asymptotic behaviour of heave added mass in the limit $\omega \to 0$ can be recovered by a single trial function with a $\ln r$-type singularity. In the low-frequency limit the sway motion of a circle is exactly represented by a $y$-dipole placed at the circle centre and, for a high frequency, the heave motion is represented by a $z$-dipole.

---

† Incidentally, the imaginary part of the radiation potentials coincides, apart from a constant factor, with the even or odd part of the diffraction potentials. This result has some bearing on the construction of the 'inner solution' in the slender-body theory; see Newman (1978).

Before roll motion is considered it seems convenient to analyse how surge, sway and heave motions can be simulated for non-circular sections. Instead of starting with more complex geometries it is worth analysing a mild distortion of a circle, an ellipse for instance. In this case the focus plays the role of the circle centre and if the ellipse major axis is horizontal, for example, a source–sink pair placed at the foci should be used to represent the sway motion. Consider now the overall fluid flow induced by the motion of a rectangular or triangular cross-section. Far from the body the fluid flow should not be very different from that induced by the motion of an *inscribed elliptical section*, although locally the presence of sharp corners may be important. In order to incorporate the effect of these geometric singularities one observes that, in essence, what they do is to make the fluid particle 'rotate' around them. So the effect of the corner can be simulated by a vortex point, placed within the body and in the corner's vicinity. Or, in short, in the variational method rectangular and triangular sections can be represented by the singularities associated with the inscribed ellipse plus vortex points placed in the neighbourhood of sharp corners. More complex geometries can then be described by a convenient combination of rectangles and triangles, and even stronger singularities (bilge keels, for example) can be properly accounted for if the vortex points are placed properly.

In this way, a pattern can be visualized allowing one to represent any desirable geometry. It remains to represent the flow induced by roll motion, but here the choice seems obvious: the rolling of the body can be grossly represented by a vortex point placed at the geometric centre of the body ($(y = 0; z = 0)$ for a surface-piercing body).

Notice, however, that a single vortex point introduces a branch cut in the fluid region and consequently infinite energy with non-zero circulation. This undesirable situation can be avoided if a system of vortices is chosen in such a way that the corresponding branch cuts are placed within the body.

For the even problems two counter-rotating vortices, with the same intensity, placed near the corners ($\pm y_c; z_c$) can be used, see figure 3(a). In this case the branch cut coincides with the dashed line $-y_c < y < y_c$. To simulate *roll motion* two vortices, with intensity $-1$ and placed at ($\pm y_0; z_0$), can be used together with a third vortex, with intensity $+2$ and placed at $(0; z_0)$, see figure 3(b). Since the geometries analysed here are of surface-piercing type, $z_0 = 0$ was used in all numerical experiments for this roll–vortex system. Finally, to simulate the rotation around sharp corners in *odd problems*, the vortex system indicated in figure 3(c) was used. Again, $z_0 = 0$ was taken here.

Summarizing, the following *four* trial functions† have been introduced: (i) $T_0^\pm(y, z)$ to simulate the diffraction solution; (ii) poles, $z$-dipoles and $y$-dipoles (or a source–sink pair), placed at the inscribed ellipse foci, to simulate surge, heave and sway induced flow; (iii) a global vortex system, placed at the geometric centre of the body, to simulate roll motion; (iv) a local vortex system, placed at the corners, to simulate the fluid rotation around these geometric singularities.

These functions can be identified with unbounded fluid singularities ($\ln r$; $y/(y^2 + z^2)^{\frac{1}{2}}$; etc.) or else with free-surface singularities. From a computational point of view the first option seems to be more economical since it avoids computing the more complex free-surface singularities; see, for instance, Yeung (1975) and Nestegård & Sclavounos (1984). In the present paper, however, deep-water free-surface singularities were used. In the discussion to follow, the variational

---

† Given a function $\tilde{T}(y, z)$ the trial function is defined by $T(y, z) = \tilde{T}(y, z) - L_0(\tilde{T}) q^\pm$, to enforce the essential condition (3.9).
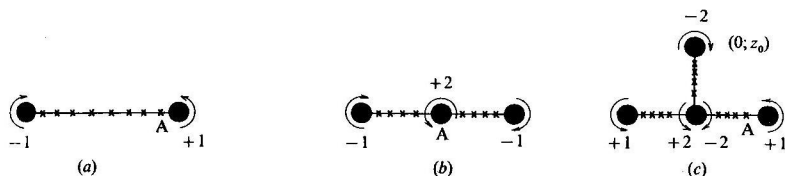
FIGURE 3. Vortex point at $A$, with branch cut and relative intensities also indicated ($z_0 = 0$ has been used in this work).

approximations will be characterized by the size of the real matrix that should be constructed and inverted or by the singularities used (one less than the size of the matrix since $T_0^{\pm}(y, z)$ has always been used). Also, an 'exact solution' means a $(10 \times 10)$ variational approximation, obtained in the way indicated in §4.1. The non-dimensional frequency is given by $\omega = K_0^{\frac{1}{2}} = \tilde{\omega}(B/2g)^{\frac{1}{2}}$, $B = $ beam.

### 4.3. *Rectangular cross-section*

Simple examples can display how an appropriate simulation of some gross flow features can improve the performance of the variational approximation. Table 3 shows a $(2 \times 2)$ approximation (one singularity) for sway and roll added mass at frequency $\omega = 0.25$. The second column is associated with a $y$-dipole placed at the origin. Since this singularity simulates neither sway nor roll motions the result is poor for both. The third column presents the results for a source–sink pair placed at the inscribed ellipse foci. Here the sway boundary condition is well simulated and the improvement for the related added mass is quite evident. The fourth column presents the result for a vortex point at the origin, see figure 3(a). Such a singularity is assumed to be a good representation of the roll boundary condition and the improvement for the related added mass is also clear.

Similar conclusions are also true for heave motion, where a single pole at the origin recovers essentially the heave added mass at frequency $\omega = 0.;25$, see the second column of table 4. At high frequency, however, the same result does not hold. A single $z$-dipole† at the origin (second column; $\omega = 2.0$) gives a poor result, with an error close to 50%. A second pole, placed at point M (see figure 2a), does not improve the result for a vortex point at the origin, see figure 3(b). Such a singularity is $\omega = 2.0$). The reason for this poor behaviour can be easily understood. As it is well known, the singularity associated with the flow around the tips of a heaving flat plate, in unbounded fluid ($\omega \to \infty$), has an important contribution to the added-mass computation. For a shallow rectangle ($B/T = 8.0$) at high frequency one should expect, then, that the flow around the sharp corners also becomes important. In order to check this a vortex point, near the corner, was used instead of M. The results shown in the fourth column of table 4 confirm this assumption – the error is now on the order of 4%, a substantial improvement. This fact seems to indicate that not only is the corner effect important for the heave mode, at high frequency, but also that the vortex point seems to be able to simulate the local feature of the flow around this point in a proper way. Once this local behaviour is properly simulated the variational method is then able to determine accurately the final result.

It should be noticed that the $(3 \times 3)_C$ approximation gives a fairly good result for both low and high frequencies and, indeed, a similar performance is observed in the

---

† A pole at the free-surface coincides, besides a constant, with a $z$-dipole, for free-surface singularities.

|       | Exact  | $(2 \times 2)_0$ | $(2 \times 2)_s$ | $(2 \times 2)_r$ |
|-------|--------|------------------|------------------|------------------|
| Sway  | 0.3574 | 0.0594           | 0.3068           | 0.1481           |
| Roll  | 0.1405 | 0.0705           | 0.0544           | 0.1244           |

TABLE 3. Effect of proper boundary condition simulation: $(2 \times 2)_0 = y$-dipole at origin; $(2 \times 2)_s =$ source–sink pair at ellipse foci (sway mode); $(2 \times 2)_r =$ vortex point at origin (roll mode). Frequency $\omega = 0.25$, rectangle with $B/T = 8.0$

| $\omega$ | Exact  | $(2 \times 2)_0$ | $(3 \times 3)_M$ | $(3 \times 3)_c$ | $(4 \times 4)$ |
|----------|--------|------------------|------------------|------------------|----------------|
| 0.25     | 6.8938 | 6.4843           | 6.7250           | 6.5473           | 6.8590         |
| 2.00     | 3.1715 | 1.8324           | 1.9493           | 3.0513           | 3.1966         |

TABLE 4. Effect of the proper simulation of the local flow field around a sharp corner. $(2 \times 2)_0 =$ pole at origin; $(3 \times 3)_M =$ pole at origin and at M; $(3 \times 3)_c =$ pole at origin plus a vortex point at corners; $(4 \times 4) =$ all three singularities. Rectangle with $B/T = 8.0$

whole range of frequencies. A $(4 \times 4)$ approximation (last column, table 4) gives essentially the 'exact' solution. Figure 4 displays the results obtained from this approximation compared with Vugts (1968), for all coefficients $\{m_{jl}; d_{jl}\}$. The agreement is excellent over the whole range of frequencies.

### 4.4. *Triangular cross-section*

Following the exposition of §4.2, the basic geometric reference for a triangle is the inscribed ellipse, with horizontal and vertical axes proportional to beam and draught, respectively. As indicated in figure 2(*b*), two corners are left: one at $(0; -\sqrt{3})$, with a 60° angle, important only for odd modes; the other at $(1; 0)$, with a 120° angle (triangle reflected on free surface), which can play a role for very high frequency.

Since the 120° corner is not so sharp the three singularities for heave motion were chosen as a $z$-dipole at the origin, a pole at ellipse focus F and another at point M. For the odd problems the singularities used were a $y$-dipole at the ellipse focus (sway), a vortex point at the origin (roll) and another at the sharp corner, see figure 2(*b*). The results obtained from this $(4 \times 4)$ variational approximation are shown in figure 5 together with those of Vugts. Again, the agreement is excellent over the whole range of frequencies.

### 4.5. *Variational approximation for* $\{T; R; Q_l\}$

So far the variational approximation has proved powerful only for the added mass and radiation damping matrices. The purpose now is to show that it is equally good in predicting the values of the exciting forces, transmission and reflection coefficients.

As will soon become clear, it suffices to show that the method is able to recover accurately the phases of $\{A_{0,5}; A_{0,6}\}$. In fact, from (3.16$a$) it follows that

$$\begin{Bmatrix} A_{0,5} \\ A_{0,6} \end{Bmatrix} = \mp \tfrac{1}{2} e^{2i\psi^{\pm}}, \tag{4.3}$$

with

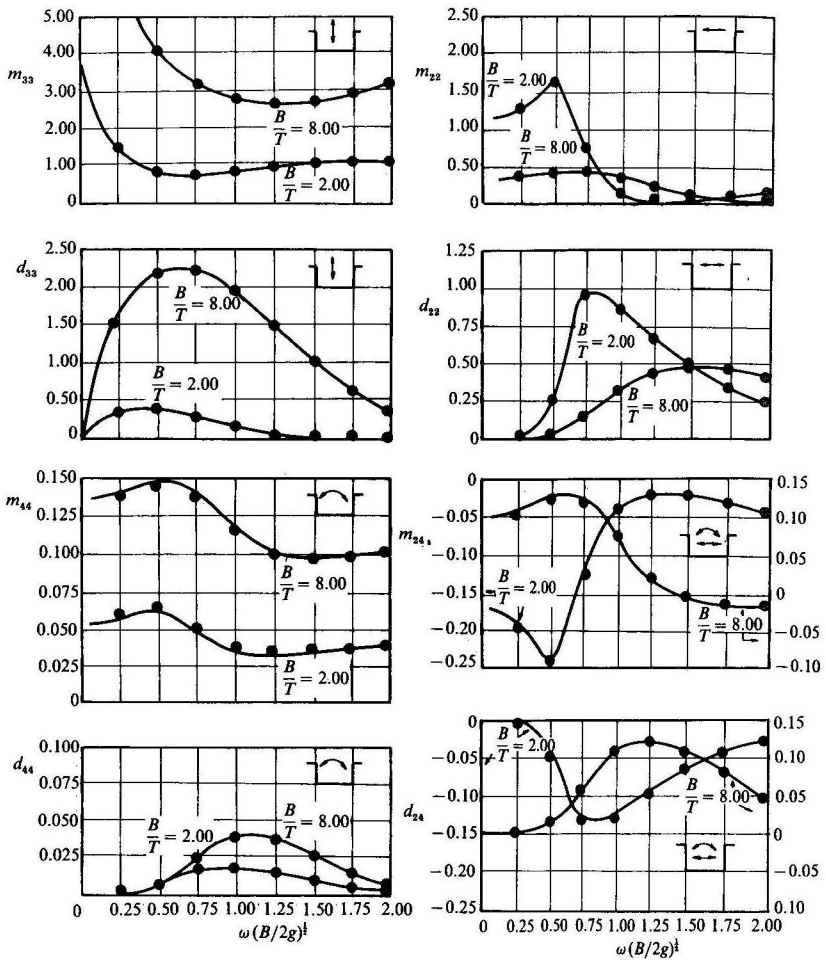$$\psi^{\pm} = \arctan \frac{K_0}{G_1(p^{\pm}; p^{\pm})}. \tag{4.4}$$

FIGURE 4. Comparison between $(4 \times 4)$ variational approximation ($\bullet$) indicated in figure $2(a)$ and Vugts' (1968) result for a rectangle (——). $\omega = \tilde{\omega}(B/2g)^{\frac{1}{2}}$; $B$ = beam.

From $(3.20b, c)$ one obtains also that

$$Q_l(\omega) = \mp i \left( \frac{K_0^3}{\omega} d_{ll}(\omega) \right)^{\frac{1}{2}} \frac{e^{i\psi\pm}}{\sin \psi^{\pm}}; \quad l = 1, \ldots, 4, \tag{4.5}$$

where $\{d_{ll}(\omega)\}$ are the diagonal terms of the radiation damping matrix. Since these coefficients can be well determined by the variational method, see §§4.3 and 4.4, and $\{T; R\}$ can be expressed directly in terms of $\{A_{0,5}; A_{0,6}\}$, see (3.6), it remains to determine the phases $2\psi \pm$.

Vugts (1968) used a different formulation and the coefficients $A_{0,5}$ and $A_{0,6}$ were not computed by him. Thus, a $(10 \times 10)$ numerical solution, as indicated in table 2,
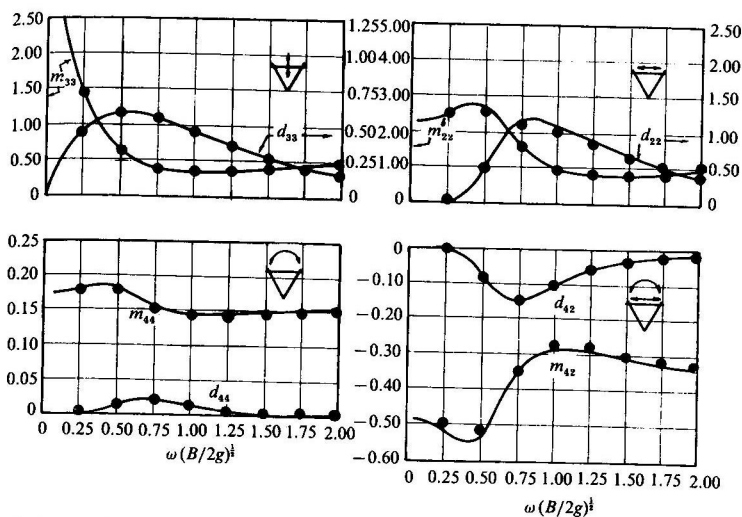
FIGURE 5. Comparison between a $(4 \times 4)$ variational approximation ($\bullet$) indicated in figure $2(b)$ and Vugts' results for an equilateral triangle (——). $\omega = \tilde{\omega}(B/2g)^{\frac{1}{2}}$; $B$ = beam.
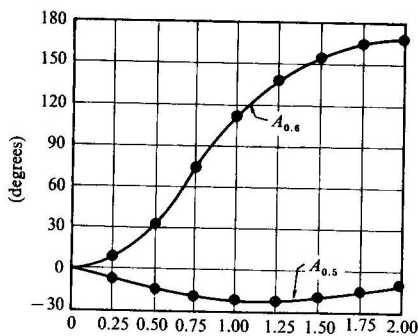


FIGURE 6. A $(4 \times 4)$ variational approximation ($\bullet$) for the phases of $A_{0,5}$ and $A_{0,6}$ indicated in figure $2(a)$, compared with the $(10 \times 10)$ solution, table 2 (——), for a rectangle with $B/T = 8.0$. $\omega = \tilde{\omega}(B/2g)^{\frac{1}{2}}$, $B$ = beam.

was used as a paradigm to test the variational approximation. As shown in figure 6, the $(4 \times 4)$ variational approximation recovers the phases of $A_{0,5}$ and $A_{0,6}$ – and so also the exciting forces, transmission and reflection coefficients – in the whole range of frequencies.

## 5. Conclusion

A variational method is developed in this paper where the relevant hydrodynamic coefficients (linear and nonlinear exciting forces, added mass and radiation damping matrices, far-field wave amplitude, drift force coefficients, etc.) are all expressed as stationary values of well-defined functionals. In this context they can be computed

6

in a similar way to which natural frequencies are computed by means of a Rayleigh quotient. As a consequence, a relatively crude approximation for the potentials can provide a much better approximation for the hydrodynamic coefficients.

As usual in variational methods (Rayleigh quotient, for example) good results can be obtained with few trial functions only if these functions simulate properly the overall behaviour of the correct solution. In this paper, combinations of simple trial functions have been introduced in such a way that they can properly simulate the overall fluid flow around an arbitrary geometry. The numerical results obtained were excellent: with a $(4 \times 4)$ symmetric real matrix all linear hydrodynamic coefficients, referring to two rectangles $(B/T = 2.0\,;8.0)$ and one triangle, were recovered over the whole range of frequencies.

Much more numerical work, however, is needed to make this method fully operational. On one hand, the use of unbounded fluid singularities, which is more economical than the standard Green-function method (see Yeung 1975; Nestegard & Sclavounous 1984), must be tested in the present variational method. The discussion on §§4.2 and 4.3 seems to indicate that they should work as well as free-surface singularities although with a greater computational efficiency (they are much simpler to be computed). Also the method itself, together with convenient trial functions, must be implemented to solve three-dimensional problems. The theory is the same but the details must be worked out.

There have been some initial applications of this method to nonlinear problems, which deserve some comments here. Aranha & Pesce (1987) have used it to estimate the effect of the second-order potential on the slow drift force acting upon a submerged body. Only one trial function was used then but the results appear to be qualitatively correct. Also, in the analysis of the nonlinear resonant response of a submerged body excited by trapped waves, a nonlinear radiation damping term appears. This coefficient can be also determined by a variational method, see Aranha (1988), and with the use of a single trial function it could be shown that this term is small for a relatively deep submerged body.

The multi-body interaction problem has also been analysed by Pesce (1988) and an extension of the present theory to related problems seems to be straightforward. For example, a problem that could be dealt with is the hydroelastic interaction between a ship hull and water waves. Also, besides some theoretical advantages, the variational method may become practically important: it can make it feasible to implement, in an efficient way, the hydrodynamic computation as a routine in a personal microcomputer. The numerical results shown here have been obtained using a standard 16-bit personal microcomputer.

## REFERENCES

ARANHA, J. A. P. 1988 Excitation of trapped waves by submerged slender structures and nonlinear resonance. *J. Fluid Mech.* **192**, 435–453.

ARANHA, J. A. P., MEI, C. C. & YUE, D. K. P. 1979 Some properties of hybrid element method for water waves. *Intl J. Num. Methods Engng* **14**, 1627–1641.

ARANHA, J. A. P. & PESCE, C. P. 1986 Effect of the second-order potential in the slow-drift oscillation of a floating structure in irregular waves. *J. Ship Res.* **30**, 103–122.

ARANHA, J. A. P. & PESCE, C. P. 1987 Slow-drift and trapping of waves on submerged bodies. *IUTAM Symp. on Non-linear Water Waves, Tokyo, August 1987.*

BESSHO, M. 1968 On boundary value problems of an oscillating body floating on water. *Mem. Defense Academy, Japan*, Vol. 8, no. 1.

LADYZHENSKAYA, O. & URAL'TSEVA, N. 1968 *Linear and Quasilinear Elliptic Equations.* Academic.

LIGHTHILL, M. J. 1979 Waves and hydrodynamic loading. *Proc. 2nd Intl Conf. Behaviour of Offshore Structures*, vol. 1, pp. 1–40. BHRA.

MOLIN, B. 1979 Second order diffraction loads upon three-dimensional bodies. *Appl. Ocean Res.* 1, 197–202.

NESTEGARD, A. & SCLAVOUNOUS, P. D. 1984 A numerical solution of two-dimensional deep water wave–body problem. *J. Ship Res.* 28, 48–54.

NEWMAN, J. N. 1978 The theory of ship motions. *Adv. Appl. Mech.* 18, 221–283.

NEWMAN, J. N., SORTLAND, B. & VINJE, T. 1984 Added-mass and damping of rectangular bodies close to the free-surface. *J. Ship Res.* 25, 219–225.

PESCE, C. P. 1988 Estudo do comportamento de corpos flutuantes em ondas: um enfoque variacional e aplicações da teoria do corpo esbelto. Doctoral thesis, Escola Politécnica da Universidade de S. Paulo (in Portuguese).

SOBOLEV, S. L. 1963 *Applications of Functional Analysis in Mathematical Physics.* Translation of Mathematical Monographs, vol. 7. American Mathematical Society.

VUGTS, J. H. 1968 The hydrodynamic coefficient for swaying, heaving and rolling cylinder in a free surface. *Int. Ship Build. Progr.* 15, 251–276.

YEUNG, R. W. 1975 A hybrid integral-equation method for time harmonic free surface flows. *Proc. 1st Intl Conf. on Numerical Ship Hydrodynamics, Gaithersburg, Md., 1975.*